

The effect of hydrodynamics on the succession of autotrophic and heterotrophic organisms of biofilms in river ecosystems

Mei Pan, Xiang Liu, Weixing Ma, Xuan Li, Haizong Li, Cheng Ding, Yuxi Chen and Runze Chen

ABSTRACT

Biofilms were cultivated for a 68-day period under different hydrodynamic conditions, and the effect of hydrodynamics on the succession of autotrophic and heterotrophic organisms of biofilms was investigated. Five obvious stages were observed during biofilm formation. At Stage I, the attachment of algae was delayed, especially under turbulent conditions. After Stage II, algal density and heterotrophic biomass of biofilms increased, which were obvious under turbulent flow. Therefore, the algal density and heterotrophic biomass of biofilms were largest under turbulent condition, followed by laminar condition, and then transitional condition. Diatoms were dominant in all flumes and were most abundant under turbulent conditions. The proportion of cyanobacteria was highest under laminar conditions. The ratio of aerobic to anaerobic bacteria decreased and their co-existence could facilitate the nitrification and denitrification in the biofilm. The ratio of monounsaturated fatty acids to saturated fatty acids was highest under turbulent conditions on the 15th day. While the ratio was highest under laminar condition on the 48th day, the high ratio indicates the high ability of biofilm to obtain nutrients, which affect the growth of algae. The regulation of hydrodynamics is a useful technology which can affect the growth of the microorganisms of biofilm, and further improve water quality.

Key words | algae, autotrophic organism, biofilm, heterotrophic organism, hydrodynamics, metabolic characteristics

HIGHLIGHTS

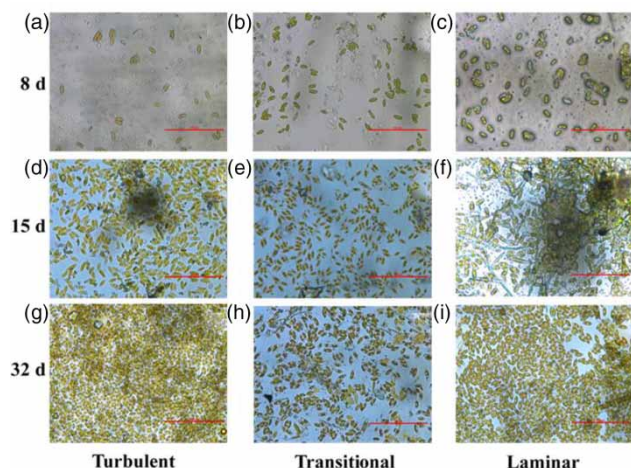
- At the initial stage of biofilm formation, algae adhesion are delayed, and the algal density and heterotrophic biomass of biofilms increase later. Both phenomena are obvious under turbulent conditions.
- High ratio of monounsaturated to saturated fatty acids indicates high ability to obtain nutrients, which affect algae growth.
- Hydrodynamics is an important factor shaping the succession of community of biofilms in rivers.

Mei Pan
Weixing Ma
Xuan Li
Cheng Ding (corresponding author)
Yuxi Chen
Runze Chen
College of Environmental Science and Engineering,
Yancheng Institute of Technology,
Yancheng 224003, Jiangsu Province,
China
E-mail: ycdingc@163.com

Xiang Liu
College of Agricultural Engineering,
Hohai University,
Nanjing 210098, Jiangsu Province,
China

Haizong Li
Yancheng Environmental Monitoring Center,
Yancheng, Jiangsu 224002,
China

GRAPHICAL ABSTRACT



INTRODUCTION

River biofilms are a complex system with very high cell density and their community structure are composed of both autotrophic organisms (e.g. diatoms, green algae, and cyanobacteria) and heterotrophic organisms (e.g. bacteria, fungi, and protozoa) (Battin *et al.* 2016). They are attached to surfaces and surrounded by their own secreted extracellular polymeric substances (EPS). Biofilm formation is usually divided into five stages according to the currently accepted model: (1) reversible adhesion of planktonic cells; (2) irreversible adhesion; (3) EPS matrix formation; (4) biofilm maturation; and (5) dispersion (Janissen *et al.* 2015). After the attachment of microorganisms to the surface, biofilms are subjected to an array of coupled physical, chemical, and biotic processes to become mature. The sufficient communication and collaboration of microorganisms in biofilms are attributed to the high diversity of microbial community structure (Flemming & Wuertz 2019).

The specific adhesion of different microorganisms to the surface and their aggregation are the prerequisites for biofilm formation and maturation (Carniello *et al.* 2018). Under the regulation of quorum sensing (QS), microorganisms adhere to the biofilm in a certain order, and the microbial distribution in biofilms is also regular and orderly, thus a complex but ordered 3-D structure is formed (Veach *et al.* 2016). The high specificity of the microorganisms in the biofilm and their ordered adhesion lead to a microbial succession process (Brislaw *et al.* 2019).

Hydrodynamics is one of the most important factors that affect the rate of transport of cells, oxygen, and nutrients to the surface of the river, and then affect the growth of biofilm and the succession of microbial community structure (Wang *et al.* 2014). However, at the same time, biofilm is a QS response to an adverse environment (higher shear stresses) to prevent the shedding of algae and bacteria, by adjusting the community structure, and its 3-D architecture (spatial arrangement of microbial cells and EPS), thickness and compactness (Risse-Buhl *et al.* 2017).

At present, there are relatively few studies on the response of autotrophic and heterotrophic organisms of river biofilm to water hydrodynamics. In this study, the succession trajectory of the effect of hydrodynamics on the biofilm community was recorded during the process of biofilm formation. The monitoring of autotrophic community structure was mainly done by evaluating the algae and chlorophyll *a*. The heterotrophic community structure was quantified using phospholipid fatty acids (PLFA) as biomarkers.

MATERIALS AND METHODS

Experimental design

The microcosms consisted of three identical Plexiglass flumes (450 cm × 8 cm × 8 cm) connected to two shared Plexiglass reservoirs (100 L, 0.5 m × 0.25 m × 0.8 m). Flumes

were designed with inlet baffles and outlet tailgates to ensure the uniform flow (Figure 1). Separate from the different flow conditions, 180 sterilized glass slides (sail brand, 75 mm × 25 mm × 1.2 mm) were placed horizontally in each flume, the biofilms were cultivated on glass slides in the three flumes, under identical nutrients and substrate conditions for ensuring the comparable basic conditions. Water recirculating in the flumes was replaced with fresh water taken from the Tongyu River (Yancheng, China) every third day, which was kept at a temperature of 15–19 °C using a thermostat. The three flumes were illuminated from above with fluorescent, cool-white tubes ($50 \mu\text{mol m}^{-2} \text{s}^{-1}$) under 12-h light/12-h dark conditions, which were controlled by a time switch socket. The hydrodynamic conditions are detailed in Table 1. The growth cycle of biofilm cultivation was 68 days, and the biofilms were collected and analyzed on the 8th, 15th, 24th, 32nd, 48th, 60th, and 68th day.

Water quality and analytical methods

Water temperature (°C), pH, dissolved oxygen (DO, mg L^{-1}) and conductivity ($\mu\text{S cm}^{-1}$) were measured with the Portable DO analyzer (HACH, HQ30d). Ammonia ($\text{NH}_4^+\text{-N}$), total phosphorus (TP), and nitrate nitrogen ($\text{NO}_3^-\text{-N}$) in water were detected using an ultraviolet (UV)–visible (Vis)

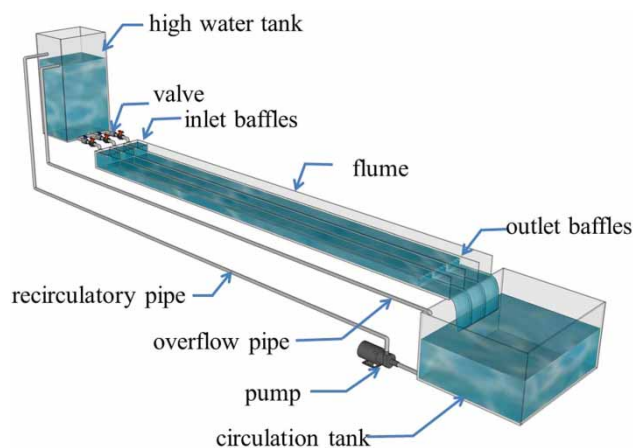


Figure 1 | 3-D-effect drawing of experimental setup.

Table 1 | Hydraulic characteristic of flumes

Hydrodynamic condition	Velocity ($\text{cm}\cdot\text{s}^{-1}$)	Reynolds (Re_f)
Turbulent	22.6 ± 1.5	$3,446 \pm 20$
Transitional	4.2 ± 0.6	653 ± 17
Laminar	1.3 ± 0.2	199 ± 12

spectrophotometer according to the national standard method (China 2002). The average conductivity was set as $429 \pm 25 \mu\text{S cm}^{-1}$, and the average DO was $5.2 \pm 0.5 \text{ mg L}^{-1}$ (\pm standard deviation, $n = 3$). Considering that the concentrations of N and P nutrients have a great effect on the growth of algae, the experiments were carried out as far as possible under a constant nutrient level in order to highlight the effect of hydrodynamics on algae. The average $\text{NH}_4^+\text{-N}$, TP, and $\text{NO}_3^-\text{-N}$ were $7.2 \pm 0.5 \text{ mg L}^{-1}$, $1.2 \pm 0.2 \text{ mg L}^{-1}$, and $8.4 \pm 0.3 \text{ mg L}^{-1}$, respectively in the river. According to their actual concentrations in the river, the amount of ammonium chloride (NH_4Cl), potassium nitrate (KNO_3), potassium dihydrogen phosphate (KH_2PO_4) were added weekly to ensure the concentrations of the three nutrients remained at a certain level.

Biofilm sample analyses

Microscopic analysis of algae and chlorophyll a

Algal morphotypes (*Navicula* diatoms, *Chlorella* and filamentous green algae, etc.) were quantified and photographed microscopically (CX31, Olympus, Japan). The results were expressed as $\text{cell}\cdot\text{cm}^{-2}$. The contents of chlorophyll a were determined spectrophotometrically with a T6 UV/Vis spectrophotometer (T6, PERSEE, China) after an acetone extraction. The final values were assessed as $\mu\text{g}\cdot\text{cm}^{-2}$ of biofilm surface area.

Extraction and identification of PLFA in biofilm

After multiple extraction steps (i.e. lipid extraction, silicic acid chromatography, and methanation) (Vinten *et al.* 2011), the identification of the extracted PLFA was carried out using the Sherlock Microbial Identification System (MIS 4.5, MIDI, Newark, Delaware, USA), which is based on fatty acid quantification of bacterial cells.

The PLFA strain identification system (Agilent 7890 gas chromatograph system and Sherlock analysis software) was used to quantify the extracted fatty acid methyl esters. The basic settings were as follows: injection volume was $2 \mu\text{L}$, the inlet temperature was $250 \text{ }^\circ\text{C}$, the detector temperature was $300 \text{ }^\circ\text{C}$, and the flow rate of the carrier gas (H_2) was 30 mL min^{-1} . The initial temperature was $170 \text{ }^\circ\text{C}$, followed by increasing by $5 \text{ }^\circ\text{C per min}$ to $260 \text{ }^\circ\text{C}$ and holding for 18 min, and then increasing the temperature $40 \text{ }^\circ\text{C per min}^{-1}$ to $300 \text{ }^\circ\text{C}$ and holding 1.5 min. Methyl nonanecane fatty acid (19:0) was used as the internal standard to calculate the absolute content of PLFAs.

The microbial community structure, that was, the abundance distribution of different groups of microorganisms, can be characterized by the distribution of characteristic fatty acids in each microbial group. In this study, only fatty acid species with a percentage greater than 1% were counted. PLFA are named as 'total carbon number: double bond number ω , and double bond distance from molecular end position', prefixes a and i represent the reverse isomerism and heterogeneity of the branch, respectively cy represents cyclopropane fatty acid; suffix c represents *cis* fatty acid; t represents a *trans* fatty acid; and 10Me represents a methyl side chain at the 10th carbon atom from the molecule end (Chowdhury & Dick 2012). The sum of all PLFA having a carbon chain length of C₁₂–C₂₀ was counted as the total amount of PLFA, which represents the total amount of microorganisms. The total amount of PLFA and the quantity of each bacterial group measured in this study were showed as absolute values. Their units were nmol·g⁻¹.

Statistical analyses

All the experiments were repeated three times, and the '±' in the data denotes standard deviation. The significance test was statistically analyzed by SPSS 19.0 (one-way analysis

of variance). $P < 0.05$ and $P < 0.01$ mean significant difference and extremely significant difference, respectively.

RESULTS AND DISCUSSION

Algal composition during the process of biofilm formation

Distribution of algae

Microscopy showed that protozoa, rotifers, and algae (most algae were diatoms, green algae, and cyanobacteria) were the main microorganisms in the sediment and the water. Diatoms, green algae, cyanobacteria, euglena, dinoflagellates, and few protozoa were the main microorganisms in the biofilms. The dominant algae in biofilms in all flumes were diatoms, which were important primary producers in water. Researchers previously pointed out that diatom genes can be bidirectionally transferred to bacteria, producing an informal recombination, and they also played an important role in nutrients allocation and environmental feedback signaling (Bowler *et al.* 2008).

Microscopic observation showed that hydrodynamics had a certain influence on the composition and quantity of algae in biofilm (Figure 2 and Table 2). In all flumes, the

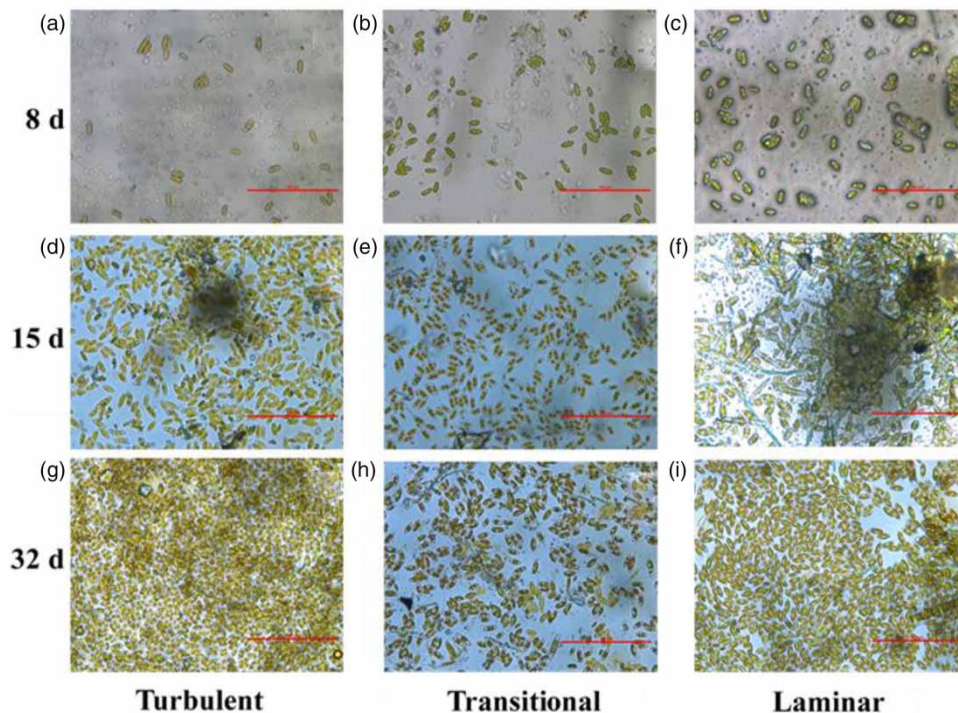


Figure 2 | Microscope photomicrographs of 8-day-old, 15-day-old, and 32-day-old biofilms formed on glass slides under turbulent, transitional, and laminar flow.

Table 2 | Algal density of biofilms in three flumes

Hydrodynamic condition	Time	Algal density (cell cm ⁻²)				
		Diatom <i>Navicula</i>	Green algae			Cyanobacteria
			<i>Chlorella</i>	Filamentous algae	<i>Scenedesmus</i>	<i>Microcystis</i>
Turbulent	8th day	10.21 ± 0.11	1.22 ± 0.05	1.05 ± 0.10	1.39 ± 0.05	1.13 ± 0.02
	15th day	100.85 ± 0.32	17.68 ± 0.08	14.97 ± 0.13	25.27 ± 0.06	25.64 ± 0.11
	32nd day	308.35 ± 1.87	40.56 ± 0.11	68.22 ± 1.13	58.20 ± 0.21	70.76 ± 0.43
	48th day	672.12 ± 9.11	70.22 ± 1.68	69.45 ± 2.14	68.32 ± 3.13	60.24 ± 1.12
Transitional	8th day	18.32 ± 0.89	3.24 ± 0.18	1.56 ± 0.31	2.45 ± 0.23	3.14 ± 0.21
	15th day	50.87 ± 0.93	16.47 ± 1.23	11.42 ± 2.21	20.22 ± 1.91	19.88 ± 0.11
	32nd day	78.32 ± 0.83	35.47 ± 2.11	70.11 ± 1.89	65.22 ± 2.56	60.22 ± 3.11
	48th day	200.89 ± 6.11	80.23 ± 2.98	90.66 ± 3.11	108.89 ± 3.31	109.79 ± 4.21
Laminar	8th day	28.33 ± 1.24	6.79 ± 0.15	4.23 ± 0.21	5.89 ± 0.41	5.28 ± 0.18
	15th day	60.25 ± 2.18	16.89 ± 1.11	20.90 ± 2.52	17.44 ± 1.51	64.32 ± 2.88
	32nd day	212.73 ± 4.28	40.22 ± 1.28	70.12 ± 2.44	60.32 ± 2.31	100.89 ± 3.01
	48th day	345.24 ± 5.11	87.23 ± 1.45	108.32 ± 1.31	90.77 ± 3.41	186.23 ± 3.21

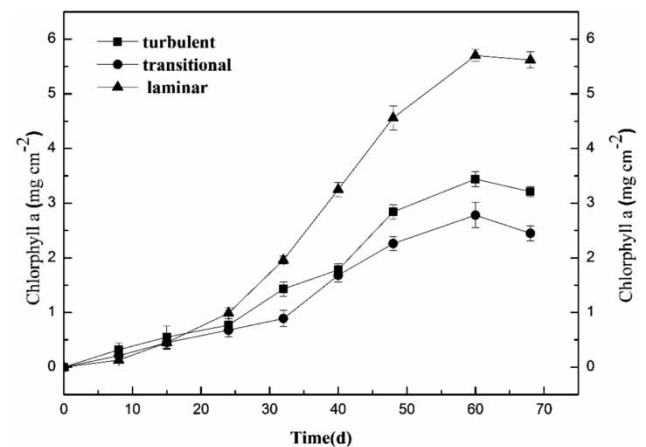
ratios of diatoms to algae were the highest, followed by green algae, while the ratio of cyanobacteria to algae of the biofilm grown in laminar flow was higher than the other two flumes (Table 2). This was consistent with the results of Li *et al.* (Li *et al.* 2013), which showed that the strength of hydrodynamic disturbance can affect the light and nutrients absorption of different algae. The results suggest that high disturbances are beneficial to diatoms and green algae, while low perturbations are beneficial to cyanobacteria. Additionally, the structure of the biofilm affects the biofilm community, especially algae due to absorption and utilization of C, N, and P.

Succession of algae during biofilm formation

Microscopy showed that the formation of biofilms had a 3–8 day stagnation, and that algae were almost not detected until after the 8th day (0–8th day is considered as Stage I) under the turbulent condition. The lag phase of biofilms under turbulent flow conditions was most obvious, which was attributed to the fastest water velocity. At Stage I, both the chlorophyll a content and algal density of biofilm were low in all flumes (Figure 2 and Table 2). A few algae were detected on the 8th day (Figure 2), with about 30–40 μm length, and almost all of them were diatoms (*Navicula* sp.).

After an initial lag phase, chlorophyll a and algae abundance steadily increased. On the 15th day, under the turbulent condition, microscopy showed that more EPS were secreted by attached algae, which in turn accelerated microbial adhesion due to the high turbulence (Figure 2).

Hence, the algal density in biofilms was highest under turbulent conditions, followed by under laminar conditions. The algae were still mainly diatoms, which secreted copious amounts extracellular polysaccharides and had less chlorophyll a content than other algae (Hoagland *et al.* 1993) (Figure 3). Previous studies also indicated that a higher flow velocity can promote the diatoms domination. Therefore, diatoms are an indicator of water quality due to their quick response to environmental changes (Rimet 2011). Because diatoms are usually small, have a large migration resistance, a fast growth rate, and a low half-saturation coefficient of nutrient absorption (Risse-Buhl *et al.* 2017), they can easily dominate biofilms in the highly dynamic habitat. For the previously-mentioned reasons, the chlorophyll a

**Figure 3** | The change curve of chlorophyll a under different hydrodynamic conditions.

content and algal density between laminar and turbulent conditions were not significantly different at this stage ($P = 0.07238$ and 0.08245 , respectively) (Figure 3, Table 2). Moreover, the distribution of diatoms was affected by the direction of water flow under the turbulent condition, which is consistent with the study by Battin *et al.* (Battin *et al.* 2003), whereas the algae distribution in laminar flow biofilms did not show significant directionality. At this stage, in addition to diatoms, the other algae, such as *Chlorella*, *Scenedesmus*, filamentous water-like genus (green algae), and *Microcystis* (cyanobacteria) also have appropriate growth under three hydrodynamic conditions. In the laminar flow flume, the distribution of algae was distinctly different from the other two, especially with more cyanobacteria (*Microcystis*) and green algae (filamentous algae), which may be due to the response of the algae to hydrodynamic conditions.

On the 32nd day, the number of algae under the turbulent conditions significantly exceeded that under the laminar conditions, and both were greater than that under the transitional conditions (Table 2). Algal cells extended away from the basal layer to form the biofilm canopy, along with EPS, other microbes, inorganic particles, and organic debris. All the morphology of biofilms were relatively dense, especially under turbulent flow conditions. The dense biofilm structure may also affect mass transfer by increasing the diffusional resistance within biofilms. Figure 2(g) and 2(i) show that, at this stage, algae were embedded in the EPS, and there were a significant accumulation stratification (the 9th–32nd day was regarded as Stage II). During this stage, biofilm morphology may be a limiting factor affecting mass transfer of DO. Oxygen plays an important role in the primary productivity and is related to the water nutrient level. Hydrodynamic disturbance promoted atmospheric reoxygenation (Risse-Buhl *et al.* 2017), and the photosynthesis of algae was the main source of DO in biofilms, which included the respiration of the biofilm and organic matter degradation in the river. The chlorophyll a of biofilms in all three flumes increased from the 24th–48th day, and the increase amplitude was the largest in the laminar flume. The content of chlorophyll a of the biofilm in the laminar flow flume was 2.5 times as much as that in the transitional flow flume.

At the beginning of the experiment, algae growth was limited, and the chlorophyll a and the number of algae at Stage I (0–8th day) were the lowest under the turbulent flow. However, from the 9th–48th day (Stage I and Stage II), they grew rapidly, which was due to the adaptation of

some algae to the environment. On the 48th day, the chlorophyll a content of biofilm under the turbulent conditions was much lower than that under the laminar conditions (approximately three-fifths) (Figure 3). Under the laminar condition, the proportion of cyanobacteria and green algae of biofilm increased (Table 2), which mainly resulted in the increase of chlorophyll a. Therefore, among the three flow conditions, the water body under the laminar flow was relatively easy to be eutrophic, further affecting the algae composition of biofilm. After the 48th day, the growth of algae in biofilms in all flumes began to slow down and, therefore, this stage of biofilm formation was Stage IV.

Hydrodynamics not only directly affected the attachment and aggregation of algae on the surface of biofilm, but it also affected the transport of nutrients and oxygen in the water to the biofilm, which in turn affected the growth of algae. In detail, flow factors such as volume and rate continually affected the transport of C, N, and P in the water to biofilms. This study shows similar results to the research of Liang *et al.* (Liang *et al.* 2013), which pointed out that hydrodynamics was the main natural factor affecting the state and process of eutrophication of river water.

Heterotrophic organism succession during biofilm formation

PLFA biomarkers and the microbial functional groups of biofilm

Quantitative and structural changes of PLFA biomarkers during the biofilm formation.

(1) Changes of PLFA biomarker species

Biofilm samples (with three parallels) were collected on the 15th, 32nd, 48th, and 60th day during the biofilm growth process under three hydrodynamic conditions. In total, 29 PLFA species (whose carbon chains have a length of 12–20) were detected, suggesting that the PLFA species in the microbial community were diverse. The detected PLFA included saturated fatty acids, branched chain fatty acids, cyclopropane fatty acids, monounsaturated fatty acids, and polyunsaturated fatty acids. The categories and characteristic peak values of the collected PLFA from the biofilm samples are listed in Tables 3 and 4, respectively.

As can be seen from Table 4, PLFA species varied during biofilm formation. At different stages of formation, the PLFA of microbial communities in biofilms were

Table 3 | Biomarker PLFA species of main functional flora

Microbial functional groups		PLFA species
Bacteria	Gram-positive bacteria (G ⁺)	14:00, i14:00, a14:00, 15:0 iso, 15:0 anteiso, 16:0 iso, 15:0 iso 3OH, 17:0 iso, 17:0 anteiso
	Gram-negative bacteria (G ⁻)	16:00, 16:1ω9c, 16:1ω7c, 16:1ω5c, 17:0 cyclo, 17:1ω8c, 18:1ω7c, cy 19:0ω8c, 18:0
Fungi		18:1ω5c, 18:3ω6c (6,9,12), 18:1ω9c, 20:1ω9c
Protozoa		20:4ω6,9,1,2,15c
Actinomycetes		19:0 10 methyl
Aerobic bacteria		a14:0, i 14:0, 15:0 2OH, 17:1ω7c, 15:0 3OH
Anaerobic bacteria		16:1ω5c, 18:00, 18:1ω7c, 18:1ω5c

different, but the overall change trends were consistent. The number of PLFA species increased during biofilm formation. Seventeen main species of PLFA in most biofilms were found on the 15th day, while 19 PLFA species were found in the turbulent condition samples. This may be because the turbulent conditions caused the secretion of more EPS and increased the adhesion of more microorganisms. Furthermore, especially at Stage II of biofilm formation, the faster flow under the turbulent condition may promote the contact of algae with biofilms, which can enhance the transport of microbes. At this stage, there was no anaerobic bacteria, and *Pseudomonas* (16:00) was the most abundant species, followed by Gram-negative bacteria (16:1ω7c), a species that existed widely in all three water flumes. On the 32nd day, the number of PLFA in the biofilm under turbulent flow increased to 24, 25 under the transitional flow, and 27 under the laminar flow. Both the biofilm samples in laminar and transitional flow flumes had more PLFA types than that in turbulent flow flumes, which was most likely because some microbes could not survive the turbulent conditions. On the 48th day, there were 25 species under turbulent flow, and 29 species under laminar and transitional flows, which were the same as the PLFA species obtained on the 60th day. Under the turbulent conditions, anaerobic bacteria (18:0 and 18:1ω7c) were detected at an earlier time than transitional and laminar conditions, which was probably because the biofilm cultures gradually became denser after 15 days, and anoxic areas appeared. In general, there were fewer biofilm species under turbulent flow conditions than under laminar and transitional flow conditions at Stages III and IV of biofilm formation.

(2) Changes in PLFA biomass during biofilm formation

The molar concentration of PLFA in all biofilms were calculated using the Sherlock MIS system's output value normalized to the internal standard methyl nonadecylate

in combination with their molar concentration. The conversion coefficient between PLFA and biomass was usually 2×10^4 – 6×10^4 cell-pmol⁻¹ PLFA (White *et al.* 1979), and 4×10^4 cell-pmol⁻¹ was used in this study. The monitoring data showed that not only the species but also the quantity of algae increased with the biofilm culture time. Both the total amount of PLFA and the content of individual species of PLFA varied with the hydrodynamic conditions and culture time (Figure 6).

At Stages III and IV of biofilm formation, the main PLFA detected were 14:0, i14:0, a14:0, 15:0 2OH, 15:0 3OH, 16:0, 16:1ω5c, 16:1ω7c, 16:1ω9c, 18:1ω9c, 18:0, 18:3ω6c (6,9,12), 20:1ω9c and 20:4ω6,9,12,15c (protozoa). These PLFAs not only represented a large proportion in total fatty acids, but were also abundant under all three conditions. The change of PLFA content was also different throughout the biofilm formation.

As showed in Figure 4, at Stages III and IV of biofilm formation, the total PLFA biomass of biofilm under turbulent conditions were all the highest: 22×10^7 cell g⁻¹ at 48th day and 18×10^7 cell g⁻¹ on the 60th day. These values were higher than their counterparts under the transition flow (15×10^7 cell g⁻¹ and 13.1×10^7 cell g⁻¹) and laminar flow (17.7×10^7 cell g⁻¹ and 13.8×10^7 cell g⁻¹). On the 32nd day, the biomass of biofilm PLFA increased rapidly compared to the 15th day. This may be because the secretion of EPS increased, which further promoted the high-speed growth of microbes from days 24 to 32. Decomposition of organic matter as a result of bacterial action and self-predation by protozoa are an important part of the food chain in nature. With the emergence of protozoa and their increase in number (as showed in Table 4), the predation effect on bacteria also increased, resulting in a reduced bacterial population. In general, the quantity of biofilms was significantly reduced under three hydrodynamic conditions at the 60th day. This stage should be the Stage V of biofilm formation.

Table 4 | Dynamic changes of the PLFA biomarkers in biofilm cultured under the control of hydrodynamics during the process of formation (biomass 10^5 cell g^{-1} biofilm)

Serial number	PLFA biomarkers	15th day			32nd day			48th day			60th day		
		Turbulent	Transitional	Laminar									
1 Bacteria	12:0 anteiso	0.00	0.00	0.00	0.00	0.00	0.00	0.00	0.32	0.22	0.00	17.52	14.06
2	12:1 at 11-12	0.00	0.00	0.00	0.00	0.00	0.03	0.00	0.00	16.36	0.00	0.00	15.44
3 Bacteria	13:0 anteiso	0.04	0.00	0.00	0.03	0.04	0.04	0.26	0.17	0.20	20.20	16.08	23.02
4	13:0 3OH	0.00	0.00	0.00	0.00	0.00	0.91	0.00	0.00	19.03	0.00	0.00	28.81
5 Bacteria	14:0	5.28	6.77	6.16	82.91	71.68	61.01	180.65	95.59	126.82	143.92	100.30	113.60
6 Aerobic bacteria G +	a14:0	3.75	4.73	3.78	81.73	73.42	58.21	136.20	76.59	89.64	91.80	66.82	70.72
7 Aerobic bacteria G +	i14:0	1.13	1.55	1.09	27.36	25.13	27.80	59.63	42.82	44.11	39.13	29.29	35.57
8 <i>Bacillus</i> G +	15:0 iso	1.08	1.24	2.70	25.09	22.90	56.16	47.53	34.22	53.72	37.69	36.48	41.77
9 Aerobic bacteria	15:0 2OH	1.73	1.94	2.92	41.64	35.72	47.67	44.23	29.85	29.70	18.58	23.41	18.89
10 Aerobic bacteria	15:0 3OH	2.95	2.53	3.08	46.55	42.08	46.55	108.26	75.53	76.30	58.43	52.18	43.29
11 G +	16:0 iso	0.00	0.00	0.00	0.11	0.17	0.14	0.26	0.32	0.27	18.40	17.39	27.71
12	16:0 anteiso	0.00	0.00	0.00	21.00	21.91	30.13	24.64	25.18	30.41	24.17	20.27	23.02
13 Anaerobic methane oxidizer G-	16:1 ω 5c	2.66	2.01	2.87	38.27	25.80	27.61	48.63	42.52	38.42	40.04	31.78	29.64
14 Bacteria G-	16:1 ω 7c	6.40	5.92	5.81	93.09	104.01	110.46	179.99	152.12	197.79	126.78	117.30	107.67
15	16:1 ω 9c	3.23	2.56	2.72	57.45	48.20	47.39	117.06	77.04	88.58	97.75	61.59	60.38
16 <i>Pseudomonas</i> G-	16:00	12.98	12.81	12.02	200.09	169.90	200.95	398.92	264.44	271.96	316.33	197.72	159.10
17	15:0 iso 3OH	0.00	0.00	0.00	0.00	0.10	0.11	0.00	7.57	19.51	0.00	9.74	14.71
18 Aerobic bacteria	17:1 ω 7c	0.00	0.00	0.00	0.01	0.01	0.01	0.26	0.35	0.55	20.02	14.91	24.40
19 G-	17:1 ω 8c	1.68	1.03	1.37	21.09	17.20	30.23	46.43	29.40	53.54	20.02	13.47	26.19
20 Fungi	18:3 ω 6c	1.23	0.97	1.03	20.36	34.31	30.41	69.09	47.19	45.53	50.14	41.98	41.08
21 Anaerobic/phagocytic hydrolysis bacillus	18:0	0.00	0.00	0.00	19.36	0.37	0.55	148.96	81.87	77.02	130.21	88.40	78.58
22 Anaerobic/ <i>Pseudomonas</i> bacteria G-	18:1 ω 7c	0.00	0.00	0.00	19.36	8.63	1.31	227.52	144.74	159.72	228.50	102.91	129.87
23 Fungi	18:1 ω 9c	3.43	3.01	3.68	81.82	67.05	76.50	229.94	153.93	207.57	164.84	95.46	111.81
24 Anaerobic bacteria G-	18:1 ω 5c	1.66	1.23	1.50	20.45	25.63	33.68	48.63	47.04	47.49	21.46	44.72	37.50
25	18:0 2OH	1.23	0.00	0.00	11.00	13.26	11.42	44.23	44.78	47.49	37.51	36.09	36.81
26 Actinomycetes	19:0 10 methyl	0.58	0.62	0.81	11.00	10.00	10.45	36.31	31.81	34.15	19.84	12.82	15.44
27 Protozoa	20:4 ω 6,9,1,2,15c	0.00	0.00	0.00	0.00	0.00	0.00	0.03	0.03	0.04	56.09	40.41	29.23
28 Fungi	20:1 ω 9c	0.00	0.00	0.00	0.09	0.09	0.20	1.76	1.51	1.60	19.48	15.95	17.92
29 <i>Burkholderia</i> G-	cy19:0 ω 8c	0.00	0.00	0.00	0.19	0.25	0.01	1.34	0.81	0.91	2.16	2.75	2.48

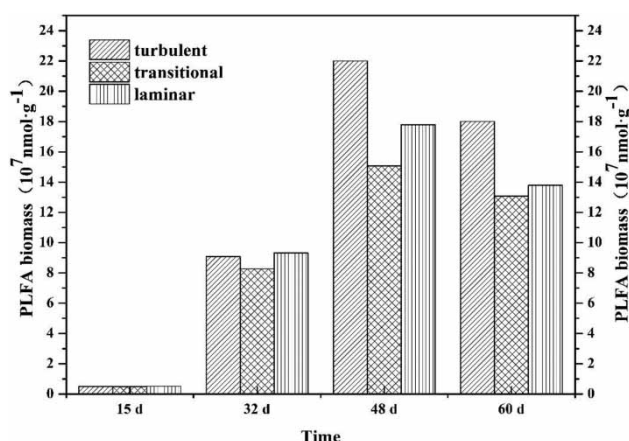


Figure 4 | Dynamic changes of the total PLFA biomass in biofilm cultured under the control of hydrodynamics during the process of formation.

(3) Changes in the structural distribution of PLFA biomarkers

Twenty-nine PLFA biomarkers were extracted from biofilm samples under different hydrodynamic conditions, indicating different types of microorganisms, such as Gram-negative bacteria, Gram-positive bacteria, fungi, aerobic bacteria, anaerobic bacteria, and protozoa, etc. The distribution of PLFA biomarkers detected in the biofilms can be divided into four categories. (1) The first category was where only a small amount of these biomarkers were found, and their distribution in biofilms cultured under different hydrodynamic conditions were not comprehensive. For example, 12:0 anteiso and 13:0 3OH (indicating bacteria) were only found in the mature biofilm under laminar condition, and their maximum percentages were about 1%. (2) The second category was where only a small amount of these biomarkers were found, but they were distributed in almost all biofilms. For example, 15:0 2OH indicating aerobic bacteria and 19:0 10 methyl indicating actinomycetes were detected in biofilm under three hydrodynamic conditions, while their content only represented about 5% and 1% of the total PLFAs, respectively. (3) The third category was that a large amount of these biomarkers were found. However, they were only distributed under certain experimental conditions. For example, 18:1 ω 7c indicating Gram-negative bacteria was not detected in the biofilm until the 15th day, while it represented 12.67% of the total amount in the late stage under the turbulent condition. (4) The last category was that a large amount of these biomarkers were found, and they were evenly distributed in all experimental settings. For example, 14:0 and 16:0 (indicating Gram-positive and negative bacteria, respectively) had overall average percentages of approximately 9% and 20% under

different growth conditions, respectively. Biomarker 16:0 can be widely found in various types of microorganisms, and it was often used to indicate total microbial biomass (Salomonová *et al.* 2003).

Changes in the quantity and structure of major microbial functional groups in biofilms

For the species of PLFA detected (Table 4), the PLFA indicated that aerobic bacteria include a14:0, i14:0, 15:0 2OH, 15:0 3OH, 17:0, and 17:0 2OH. The PLFA indicated that anaerobic bacteria include 16:1 ω 5c, 18:0, 18:1 ω 5c and 18:1 ω 7c. The PLFA also indicated that fungi include 18:3 ω 6c, 18:1 ω 9c and 20:1 ω 9c; for actinomycetes, the featured PLFA was 19:0 10 methyl; and for protozoa, the featured PLFA was 20:4 ω 6,9,1,2,15c (Table 3).

Under different hydrodynamic conditions, Figure 5 shows that of the major microbial functional groups in biofilms, the bacteria were always the largest functional groups in biofilms, with a percentage was greater than 80% (the highest percentage was 86%). Aerobic bacteria decreased from approximately 20% to 13%. The proportion of anaerobic bacteria under turbulent conditions increased from 8% to 23%, and its total amount ranged from $4.32 \times 10^5 \text{ cell g}^{-1}$ to $4.20 \times 10^7 \text{ cell g}^{-1}$ biofilm on the 60th day, which was relatively high compared to that under the other two conditions. This was probably due to the different biofilm density caused by turbulent flow. Under turbulent conditions, on the 15th and 32nd day, the percentages of protozoa were 0% and 0%, respectively, which increased to 3% on the 60th day. Under transitional conditions, on the 15th and 32nd day, the percentages of protozoa were 0% and 0%, respectively, which increased to 2% on the 60th day. In the mature biofilm (when cultured for 60 days), the order of functional groups under each condition from large percentage to small percentage were as follows: under the turbulent flow condition, bacteria > protozoa > anaerobic bacteria > fungi > aerobic bacteria > actinomycete; under both transitional and laminar flow conditions: bacteria > protozoa > anaerobic fungi > fungi > aerobic bacteria > actinomycetes. The significant increase in protozoa explains the overall reduction in microbial population.

Dynamic distribution of characteristic of PLFA in biofilms

In this study, the detected PLFA included saturated fatty acids, branched saturated fatty acids, monounsaturated fatty acids, polyunsaturated fatty acids, and cyclopropane fatty acids (see Table 5 for the details). Their contents

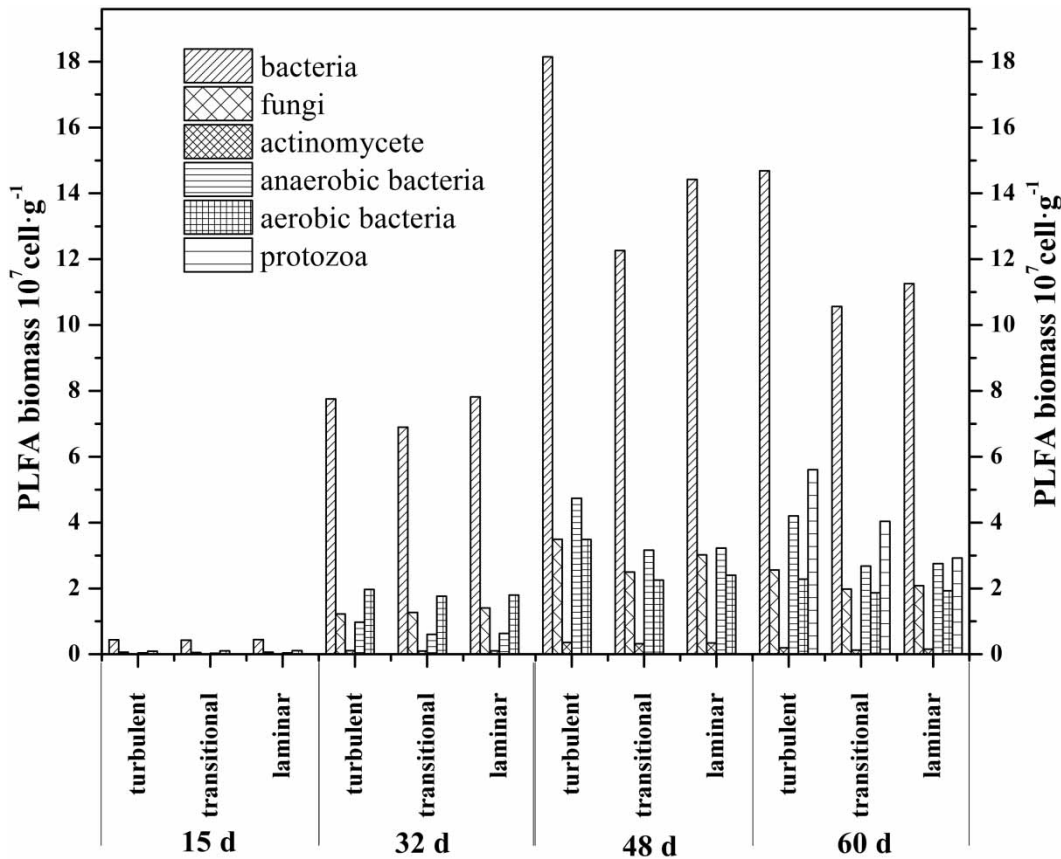


Figure 5 | Dynamic changes of the total biomass of functional bacteria groups in biofilms cultured under different hydrodynamic conditions during the process of formation.

Table 5 | List of characteristic PLFA in the biofilm

Serial number	Fatty acid species	Fatty acid
1	Saturated fatty acids	14:00, 16:00, 18:00
2	Branched saturated fatty acids	a14:0, i14:0
3	Monounsaturated fatty acids	16:1 ω 5c, 16:1 ω 7c, 16:1 ω 9c, 17:1 ω 7c, 17:1 ω 8c, 18:1 ω 5c, 18:1 ω 7c, 18:1 ω 9c, 20:1 ω 9c
4	Polyunsaturated fatty acids	18:3 ω 6c, 20:4 ω 6,9,1,2,15c
5	Cyclopropane fatty acids	cy19:0 ω 8c

accounted for 25.12–36.48%, 7.51–12.84%, 32.24–44.71%, and 1.98–6.3% of the total PLFA, respectively; cyclopropane fatty acid ($2.75 \times 10^5 \text{ cell g}^{-1}$) only represented a small fraction (0.1%) of the total PLFA (data not shown). The other PLFA data are shown in Figure 6.

At any certain sampling time, saturated fatty acids, monounsaturated fatty acids, branched saturated fatty acids and polyunsaturated fatty acids in the biofilm under turbulent flow condition were all more abundant than under the other two hydrodynamic conditions. Therefore, the dynamic variation of PLFA content from the 15th to 48th day is related to enhanced adhesion of microbes because of higher EPS amount. The ratio of monounsaturated fatty acids to saturated fatty acids in all flow conditions was approximately 1, and most of them were between 1 to 2 (Table 6).

Effect of microbial community structure on the metabolic characteristics of biofilms

PLFA not only provide information on the microbial community structure, but also give clues on the state of microbial metabolism. The ratio of characteristic PLFA can be used to explore the metabolic properties of the microbial community structure (Li et al. 2010).

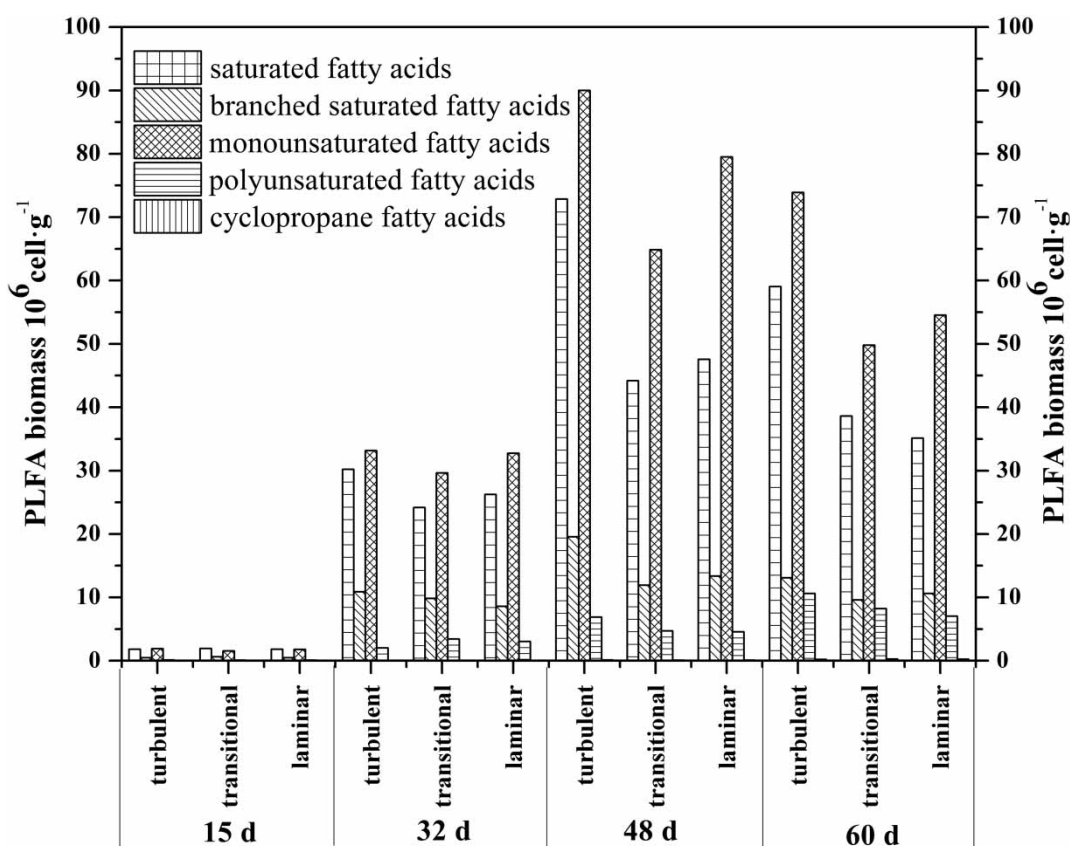


Figure 6 | Dynamic changes of the total content of characteristic PLFA in biofilm cultured under the control of hydrodynamics during the process of formation.

Table 6 | Ratios of monounsaturated to saturated PLFAs and aerobic to anaerobic bacteria

Culture time	Monounsaturated fatty acid: saturated fatty acid			Ratio of aerobic: anaerobic bacteria		
	Turbulent	Transitional	Laminar	Turbulent	Transitional	Laminar
15th day	1.04 ± 0.02 ^b	0.80 ± 0.05 ^c	0.98 ± 0.04 ^d	2.21	3.32	2.49
32nd day	1.09 ± 0.03 ^b	1.22 ± 0.04 ^b	1.25 ± 0.03 ^c	2.02	2.92	2.85
48th day	1.24 ± 0.05 ^a	1.46 ± 0.08 ^a	1.67 ± 0.02 ^a	0.74	0.71	0.74
60th day	1.25 ± 0.04 ^a	1.29 ± 0.03 ^b	1.55 ± 0.03 ^b	0.54	0.70	0.70

Note: Different letters in the same column are statistically significant ($P < 0.05$); as described in Wadige *et al.* (2014).

Effects of the ratios of monounsaturated to saturated PLFAs on biological metabolic properties

The ratio of monounsaturated fatty acids to saturated fatty acids is an indicator of physiological or nutritional stress in the microbial community. This ratio is usually low when organic carbon and/or nutrient sources are insufficient for microorganisms (Gomez-Brandon *et al.* 2011). As can be seen from Table 6, the ratio of monounsaturated

fatty acids to saturated fatty acids increased with the prolongation of culture time under all three conditions. This was probably due to a growing number of species and quantity of microbes. They secreted more enzymes which gradually promote organisms to decompose high-molecular organic molecules from the surrounding water into simple and absorbable low-molecular-weight nutrients.

The ratio was highest under the turbulent conditions on the 15th day (ratios were 1.04 under turbulent conditions,

0.8 under transition conditions, and 0.98 under laminar conditions). A possible reason for this may be because the highest EPS content in the biofilm was under the turbulent condition during this period. The early attached microbes preferred to use their own secreted EPS as the carbon source for growth (Pohlen *et al.* 2010). However, under the turbulent conditions, at the latter stages of biofilm formation, the ratio of the two types of fatty acids did not increase significantly. This may be due to a higher bacterial density in the turbulent flow flume, which mostly constrained the mass transfer of nutrients, resulting in a relatively reduced rate of nutrient utilization. Under the transitional condition, the ratio of the two types of biofilm fatty acids increased from 0.8 on the 15th day to 1.22 on the 32nd day (Stage II), which was the largest increase among the three flumes. Similarly, this was mainly because the adhesive speed was the slowest among the three conditions, and the biofilm morphology was the loosest at this stage. However, on the 48th day, the ratio was the highest under the laminar conditions (ratios were 1.24 under turbulent conditions, 1.46 under transition conditions, and 1.67 under laminar conditions). This is mostly because that with high thickness, loose interior, and abundant biomass of biofilm, microbes in the biofilm are able to uptake nutrients easily. This was consistent with the previous conclusion that the species and number of algae were affected by nutrients. Under laminar conditions, the ratio of monounsaturated fatty acids to saturated fatty acids was higher, indicating that the ability of biofilm to obtain nutrients was relatively greater. In turn, the nutrients in the biofilm affected the growth species and number of algae in the biofilm, and there were more cyanobacteria in the biofilm under laminar conditions. Under all three conditions, the ratio of two biofilm fatty acids were lower on the 60th day than at any other time before, because of the emergence of protozoa. They reduced the abundance of microbes in the biofilms and restricted the utilization of DO when biodegrading organic matters.

Effect of the ratio of aerobic/anaerobic bacterial PLFAs on biological metabolic properties

According to Zhao *et al.* (Zhao *et al.* 2014), the ratio of aerobic:anaerobic bacterial PLFA was usually greater than 1.00, indicating an advantage of aerobic microorganisms. As showed in Table 6, during the biofilm formation process, the ratio of aerobic:anaerobic bacterial PLFA decreased because the morphology of the biofilm changed continuously, and the population of some anaerobic bacteria

surpassed aerobic bacteria with the increase of biofilm thickness and density. The aerobic:anaerobic bacteria ratio in all three flumes decreased significantly from the 32nd to 48th day period (Stage III), which may be attributed to the sharp increase of biofilm EPS. This increase probably led to a denser biofilm structure. The microbial adhesion after 32 days was also promoted by the rapid increase of EPS. This was coupled with the limited transfer of DO in the biofilm, which benefited the growth of anaerobic bacteria. On the 60th day, the ratio was slightly lower, which may be caused by the predation of protozoa. In addition, the ratio of aerobic:anaerobic bacteria in the transitional flow biofilm on the 15th day was highest, because there was less biofilm adhesion and sufficient DO to facilitate the adhesion of aerobic organisms. The co-existence of anaerobic and aerobic bacteria is beneficial to the nitrification and denitrification of microbes in biofilm, which further promotes the removal of N in water (He *et al.* 2018).

CONCLUSION

Five stages were observed in this study. Day 0–8 can be considered as Stage I of biofilm formation, followed by Stage II (9th–32nd day), Stage III (32nd–48th day), Stage IV (48th–60th day), and Stage V (60th–68th day). Under three hydrodynamic conditions and at Stage I of biofilm formation, algae that were attached to carriers had an evident stasis period. After Stage II, the adhesion of algae was most obvious under the turbulent flow. The algal density of biofilm under turbulent conditions was largest, followed by laminar conditions, and then transitional conditions. Diatoms were dominant, which were most abundant under turbulent conditions. In addition, the proportion of cyanobacteria and green algae in the biofilm under the laminar conditions were higher than the other two conditions, and the content of cyanobacteria and chlorophyll a was lowest under the turbulent conditions. All these suggest that turbulent flow obviously inhibited the proliferation of cyanobacteria in biofilms.

The species and biomass of heterotrophic organisms in biofilms increased with the formation of biofilms. After Stage II, the biomass in dense biofilms under turbulent flow was the highest (on the 48th day, under the turbulent flow, it was 1.46 and 1.24 times more than under the laminar and transitional flows, respectively). The quantity of bacteria under different hydrodynamic conditions was different, while bacteria were always the largest proportion of functional bacteria in biofilms.

With the formation of biofilms, the ratio of monounsaturated fatty acids to saturated fatty acids in biofilms increased to varying degrees. The high ratio indicates the high ability of the biofilm to obtain nutrients, which affects the growth of algae. That may be why there was relatively more cyanobacteria in the biofilm in the laminar flume than in the two other flumes. In addition, with the formation of biofilms, anaerobic bacteria first appeared under the turbulent flow. The ratio of aerobic bacteria to anaerobic bacteria showed a decreasing trend under the three hydrodynamic conditions (from 2.0–3.0 on the 15th day to about 0.7 on the 48th day). The co-existence of anaerobic and aerobic bacteria may facilitate the nitrification and denitrification of organisms in biofilm, which can further promote the removal of N in water.

ACKNOWLEDGEMENTS

The authors appreciate the support of the National Natural Science Fund of China (grant numbers: 51608466 and 51808480). The authors also want to thank Yin Su who provided for helpful suggestions and corrections on the earlier draft of our study according to which we improved the content.

DATA AVAILABILITY STATEMENT

All relevant data are included in the paper or its Supplementary Information.

REFERENCES

- Battin, T. J., Kaplan, L. A., Newbold, J. D., Cheng, X. & Hansen, C. 2003 *Effects of current velocity on the nascent architecture of stream microbial biofilms*. *Applied and Environmental Microbiology* **69**, 5443–5452. doi:10.1128/AEM.69.9.5443-5452.2003.
- Battin, T. J., Besemer, K., Bengtsson, M. M., Romani, A. M. & Packmann, A. I. 2016 *The ecology and biogeochemistry of stream biofilms*. *Nature Reviews Microbiology* **14**, 251–263. doi:10.1038/nrmicro.2016.15.
- Bowler, C., Allen, A. E., Badger, J. H., Grimwood, J., Jabbari, K., Kuo, A., Maheswari, U., Martens, C., Maumus, F., Otilar, R. P., Rayko, E., Salamov, A., Vandepoele, K., Beszteri, B., Gruber, A., Heijde, M., Katinka, M., Mock, T., Valentin, K., Verret, F., Berges, J. A., Brownlee, C., Cadoret, J. P., Chiovitti, A., Choi, C. J., Coesel, S., De Martino, A., Detter, J. C., Durkin, C., Falciatore, A., Fournet, J., Haruta, M., Huysman, M. J., Jenkins, B. D., Jiroutova, K., Jorgensen, R. E., Joubert, Y., Kaplan, A., Kroger, N., Kroth, P. G., La Roche, J., Lindquist, E., Lommer, M., Martin-Jezequel, V., Lopez, P. J., Lucas, S., Mangogna, M., McGinnis, K., Medlin, L. K., Montsant, A., Oudot-Le Secq, M. P., Napoli, C., Obornik, M., Parker, M. S., Petit, J. L., Porcel, B. M., Poulsen, N., Robison, M., Rychlewski, L., Rynearson, T. A., Schmutz, J., Shapiro, H., Siaut, M., Stanley, M., Sussman, M. R., Taylor, A. R., Vardi, A., von Dassow, P., Vyverman, W., Willis, A., Wyrwicz, L. S., Rokhsar, D. S., Weissenbach, J., Armbrust, E. V., Green, B. R., van de Peer, Y. & Grigoriev, I. V. 2008 *The *Phaeodactylum* genome reveals the evolutionary history of diatom genomes*. *Nature* **456**, 239–244. doi:10.1038/nature07410.
- Brislawn, C. J., Graham, E. B., Dana, K., Ihardt, P., Fansler, S. J., Chrisler, W. B., Cliff, J. B., Stegen, J. C., Moran, J. J. & Bernstein, H. C. 2019 *Forfeiting the priority effect: turnover defines biofilm community succession*. *ISME Journal* **13**, 1865–1877. doi:10.1038/s41396-019-0396-x.
- Carniello, V., Peterson, B. W., van der Mei, H. C. & Busscher, H. J. 2018 *Physico-chemistry from initial bacterial adhesion to surface-programmed biofilm growth*. *Advances in Colloid and Interface Science* **261**, 1–14. doi:10.1016/j.cis.2018.10.005.
- China EPA 2002 *Environmental Quality Standards for Surface Water*. MEP, China, Beijing GB3838-2002.
- Chowdhury, T. R. & Dick, R. P. 2012 *Standardizing methylation method during phospholipid fatty acid analysis to profile soil microbial communities*. *Journal of Microbiological Methods* **88**, 285–291. doi:10.1016/j.mimet.2011.12.008.
- Flemming, H. C. & Wuertz, S. 2019 *Bacteria and archaea on Earth and their abundance in biofilms*. *Nature Reviews Microbiology* **17** (4), 247–260. doi:10.1038/s41579-019-0158-9.
- Gomez-Brandon, M., Aira, M., Lores, M. & Dominguez, J. 2011 *Changes in microbial community structure and function during vermicomposting of pig slurry*. *Bioresour Technol* **102**, 4171–4178. https://doi.org/10.1016/j.biortech.2010.12.057.
- He, Q., Yin, F., Li, H., Wang, Y., Xu, J. & Ai, H. 2018 *Suitable flow pattern increases the removal efficiency of nitrogen in gravity sewers: a suitable anoxic and aerobic environment in biofilms*. *Environmental Science and Pollution Research* **25** (16), 15743–15753. doi:10.1007/s11356-018-1768-x.
- Hoagland, K. D., Rosowski, J. R., Gretz, M. R. & Roemer, S. C. 1993 *Diatom extracellular polymeric substances: function, fine structure, chemistry, and physiology*. *Journal of Phycology* **29**, 537–566. doi:10.1111/j.0022-3646.1993.00537.x.
- Janissen, R., Murillo D, M., Niza, B., Sahoo, P. K., Nobrega, M. M., Cesar, C. L., Temperini, M. A., Carvalho, H. F., de Souza, A. A. & Cotta, M. A. 2015 *Spatiotemporal distribution of different extracellular polymeric substances and filamentation mediate *Xylella fastidiosa* adhesion and biofilm formation*. *Scientific Reports* **5**, 1–10. doi:10.1038/srep09856.
- Li, M., Zhou, Q., Tao, M., Wang, Y., Jiang, L. & Wu, Z. 2010 *Comparative study of microbial community structure in different filter media of constructed wetland*. *Journal of*

- Environmental Sciences* **22**, 127–133. [https://doi.org/10.1016/S1001-0742\(09\)60083-8](https://doi.org/10.1016/S1001-0742(09)60083-8).
- Li, F., Zhang, H., Zhu, Y., Xiao, Y. & Chen, L. 2013 **Effect of flow velocity on phytoplankton biomass and composition in a freshwater lake**. *Science of the Total Environment* **447**, 64–71. <https://doi.org/10.1016/j.scitotenv.2012.12.066>.
- Liang, P., Wang, X. & Ma, F. 2013 **Effect of hydrodynamic conditions on water eutrophication: a review**. *Journal of Lake Sciences*. **25**, 455–462. doi:10.18307/2013.0401.
- Pohlon, E., Marxsen, J. & Küsel, K. 2010 **Pioneering bacterial and algal communities and potential extracellular enzyme activities of stream biofilms**. *FEMS Microbiology Ecology* **71**, 364–373. <https://doi.org/10.1111/j.1574-6941.2009.00817.x>.
- Rimet, F. 2011 **Recent views on river pollution and diatoms**. *Hydrobiologia* **683**, 1–24. doi:10.1007/s10750-011-0949-0.
- Risse-Buhl, U., Anlanger, C., Kalla, K., Neu, T. R., Noss, C., Lorke, A. & Weitere, M. 2017 **The role of hydrodynamics in shaping the composition and architecture of epilithic biofilms in fluvial ecosystems**. *Water Research* **127**, 211–222. <https://doi.org/10.1016/j.watres.2017.09.054>.
- Salomonová, S., Lamačová, J., Rulík, M., Rolčík, J., Čáp, L. & Bednář, P. 2003 **Determination of phospholipid fatty acids in sediments**. *X-Ray Spectrometry* **30**, 49–55. <https://link.springer.com/article/10.1007/BF00336146>.
- Veach, A. M., Stegen, J. C., Brown, S. P., Dodds, W. K. & Jumpponen, A. 2016 **Spatial and successional dynamics of microbial biofilm communities in a grassland stream ecosystem**. *Molecular Ecology* **25**, 4674–4688. <https://doi.org/10.1111/mec.13784>.
- Vinten, A. J. A., Artz, R. R. E., Thomas, N., Potts, J. M., Avery, L., Langan, S. J., Watson, H., Cook, Y., Taylor, C., Abel, C., Reid, E. & Singh, B. K. 2011 **Comparison of microbial community assays for the assessment of stream biofilm ecology**. *Journal of Microbiological Methods* **85**, 190–198. <https://doi.org/10.1016/j.mimet.2011.03.001>.
- Wadige, C. P. M. M., Taylor, A. M., Maher, W. A., Ubrihien, R. P. & Krikowa, F. 2014 **Effects of lead-spiked sediments on freshwater bivalve, *Hydrilla australis*: linking organism metal exposure-dose-response**. *Aquatic Toxicology* **149**, 83–93. doi:10.1016/j.aquatox.2014.01.017.
- Wang, C., Miao, L., Hou, J., Wang, P., Qian, J. & Dai, S. 2014 **The effect of flow velocity on the distribution and composition of extracellular polymeric substances in biofilms and the detachment mechanism of biofilms**. *Water Science and Technology* **69** (4), 825–832. doi:10.2166/wst.2013.785.
- White, D. C., Davis, W. M., Nickels, J. S., King, J. D. & Bobbie, R. J. 1979 **Determination of the sedimentary microbial biomass by extractable lipid phosphate**. *Oecologia* **40**, 51–62. doi:10.1007/BF00388810.
- Zhao, C., Xing, M., Yang, J., Lu, Y. & Lv, B. 2014 **Microbial community structure and metabolic property of biofilms in vermifiltration for liquid-state sludge stabilization using PLFA profiles**. *Bioresource Technology* **151**, 340–346. <https://doi.org/10.1016/j.biortech.2013.10.075>.

First received 12 May 2020; accepted in revised form 21 October 2020. Available online 6 November 2020